Article

Role of the Environment Polarity on the Photophysical Properties of Mesogenic Hetero-Polymetallic Complex

Adelina A. Andelescu , Angela Candreva , Evelyn Popa , Alexandru Visan , Carmen Cretu , Massimo La Deda * , Elisabeta I. Szerb *

Posted Date: 7 December 2023

doi: 10.20944/preprints202312.0457.v1

Keywords: hetero-polymetallic coordination complexes; metallomesogens; emissive materials

doi:10.20944/preprints202312.0457.v1

Article

Role of the Environment Polarity on the Photophysical Properties of Mesogenic Hetero-Polymetallic Complex

Adelina A. Andelescu [1], Angela Candreva [2], Evelyn Popa [1], Alexandru Visan [1], Carmen Cretu [1], Massimo La Deda [2,3,*] and Elisabeta I. Szerb [1,*]

[1] "Coriolan Drăgulescu" Institute of Chemistry, Romanian Academy, 24 Mihai Viteazu Bvd. 3200-Timisoara, Romania; ict@acad-icht.tm.edu.ro
[2] Department of Chemistry and Chemical Technologies, University of Calabria, 87036 Rende, Italy
[3] Institute of Nanotechnology (NANOTEC), National Research Council (CNR), UOS Cosenza, 87036 Rende, Italy
* Correspondence: eszerb@acad-icht.tm.edu.ro; massimo.ladeda@unical.it

Abstract: New hetero-polynuclear coordination complexes based on pentacoordinated Zn(II) metal center with tridentate terpyridine-based ligands and monoanionic gallates functionalized with long alkyl chains containing ferrocene units were designed, synthesized and characterized by spectroscopic and analytical methods. The complexes are mesomorphic, exhibiting columnar hexagonal mesophases at room temperature. The photophysical properties in solution and in ordered condensed state were accurately investigated and the influence of the polarity of the media in solution was evidenced.

Keywords: hetero-polymetallic coordination complexes; metallomesogens; emissive materials

1. Introduction

Emissive materials containing cheap biocompatible and bioavailable *d*-block metals like copper and zinc are considered promising in several applications such as in optoelectronic devices [1–3], sensing [4–6], multi-stimuli responsive materials [7–11] and so on. The interest arises from the possibility of harvesting triplet excited states resulting into an exponential increase of emission when comparing with organic low-molecular-weight luminophores. For use in optoelectronic devices, the possibility of having luminophores capable of forming liquid-crystalline phases presents a great advantage, due to the possibility of forming films and regulating their properties through the application of electric fields [11,12].

Luminescent compounds in solution can undergo important changes in their photophysical properties when they form condensed phases, such as mesophases; in particular, these variations can be attributed to aggregation phenomena (which involve the formation of excimers or actual stacked systems which profoundly modify the emissive electronic states) [12] and/or to the variation in environmental polarity passing from the solution phase to the condensed one. Generally, this last aspect is rather neglected when the photophysics of mesogenic molecules is studied and compared with that observed in solution.

2,2′:6′,2″-terpyridine (*tpy*) and its derivatives are important chelating ligands in coordination and supramolecular chemistry yielding complexes with excellent electronic, optical and electrochemical properties [13–20]. Their coordination complexes based on the cheap biocompatible and bioavailable Zn(II) metal center were successfully used for obtaining polarized emission[21] and emissive materials for optoelectronics and luminescence-based technologies[22,23], sensing and detection [24–33], DNA binding and/or cleavage agents[34–37], bioimaging [38–40].

Increasing complexity of the molecular structure by introducing a second metal center and increasing nuclearity may induce new synergistic properties of the photophysical, electrochemical or sensing properties. Hence, we decided to synthesize complexes **Zn_1Fe_2** and **Zn_2Fe_4** (see Figure 1) and investigate their photophysical and mesogenic properties; the parent compound **Zn1**, previously described [21], is reported here for comparison.

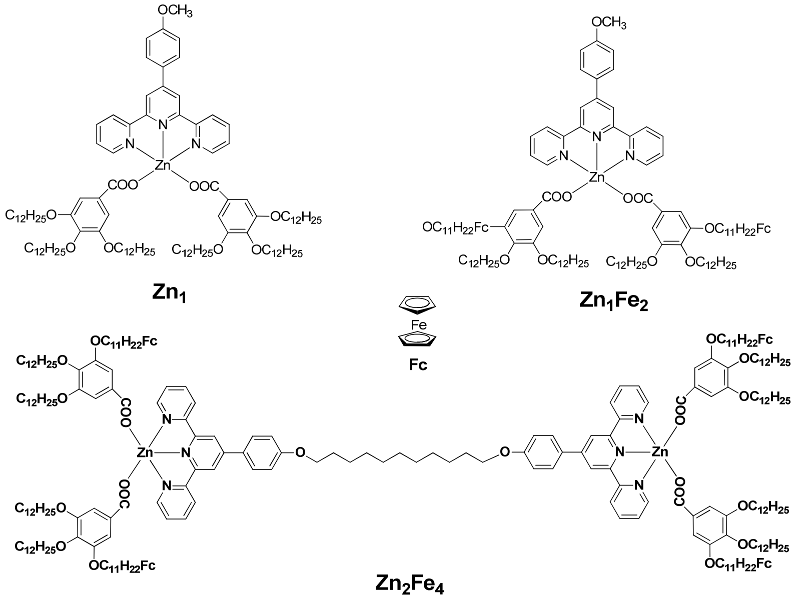

Figure 1. Molecular structure of Zn(II) *tpy*-based coordination complexes under study.

2. Results

The complexes were obtained as previously reported (see Supporting Information - SI) [19]. Their structure and purity were determined by spectroscopic (FT-IR, ^{1}H NMR, atomic absorption spectroscopy) and analytic (elemental analysis) methods, while the mesomorphic properties were assessed by polarized optical microscopy (POM) and differential scanning calorimetry (DSC) techniques. Emission maxima was followed in different polarity solutions and mixtures of solvents for determining the influence of supramolecular structures and molecular environment on the photophysical properties. Moreover, for the Zn_2Fe_4 the photophysical properties in the ordered phase were also conducted.

2.1. Synthesis and structural characterisation

The synthesis of the ligands and complexes was carried out following methods described in literature (Schemes 1 and 2) [19,41,42].

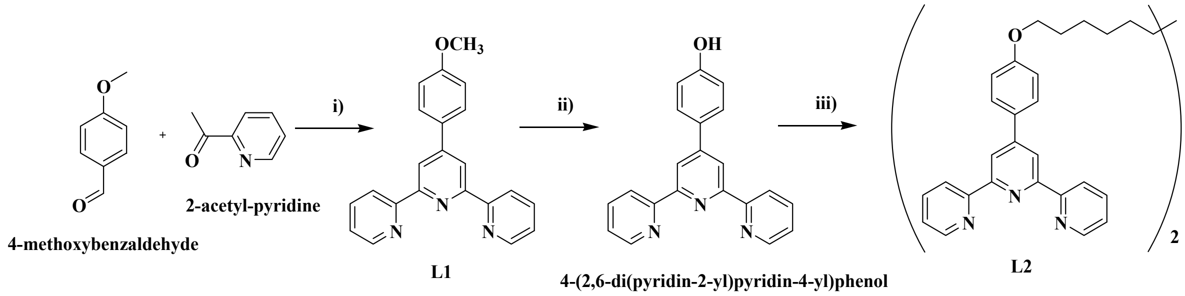

Scheme 1. Synthetic pathway for **L1** and **L2**. Conditions: i) KOH, NH_4OH, EtOH, ΔT, 24 h; ii) CH_3COOH/ HBr, ΔT, 24 h; iii) K_2CO_3, DMF, 80°C, 24 h.

Ligand **L1** was obtained by a one-pot Kröhnke condensation between 4-methoxybenzaldehyde and 2-acetylpyridine, in a basic media [41,42]. Ligand **L2** was obtained from **L1** after demethoxylation to the hydroxyl form under strong acidic conditions and isolation of this intermediate by a Williamson etherification procedure.

doi:10.20944/preprints202312.0457.v1

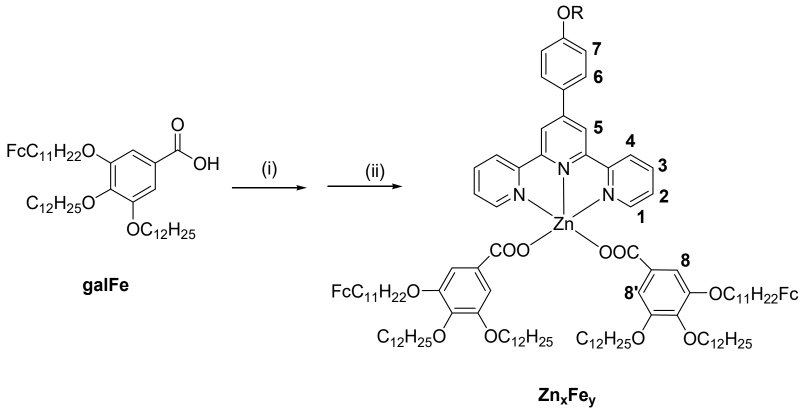

Scheme 2. Synthetic pathway for complexes **$ZnFe_2$** and **Zn_2Fe_4**. Conditions: (i) NaOH, 30 min, EtOH, then $ZnCl_2$ in EtOH, r.t., 24h; (ii) L_n, $CHCl_3$, 24h.

As for the analogues Zn(II) complexes previously reported [19,21], the pentacoordination around Zn is fulfilled by a *tpy* chelating center and two monodentate units of gallate derivative. The successful coordination was firstly assessed by FT-IR spectroscopy, by the significant shift to higher frequencies of the $\nu_{C=C}$ and $\nu_{C=N}$ ligand characteristic bands (Figure 2a,b) and the monodentate coordination mode of the gallate units evidenced by the separation of the stretching vibrations of COO^- group: $\Delta \approx 260$ cm^{-1} [43]. The purity of the final complexes was assessed by elemental analysis and atomic absorption spectroscopy (AAS – Experimental Section).

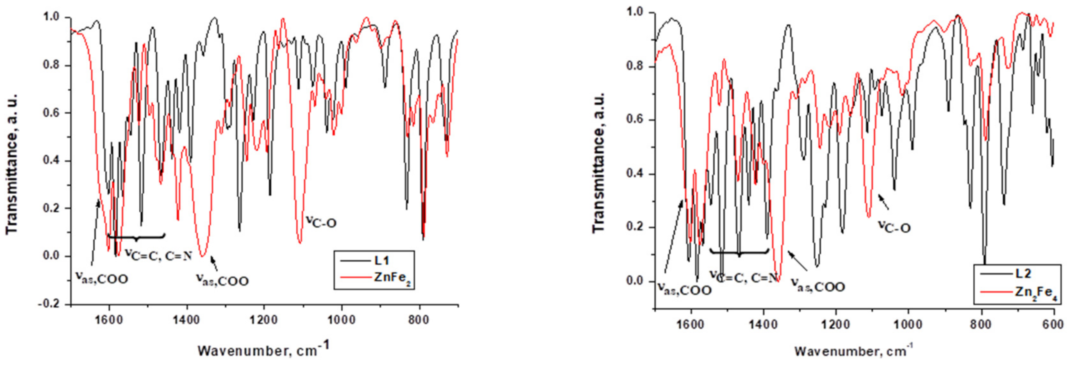

(**a**) (**b**)

Figure 2. FT-IR spectra of (**a**) ligand **L1** and complex **Zn_1Fe_2** and (**b**) **L2** and complex **Zn_2Fe_4** with the principal absorption bands evidenced.

2.2. Mesomorphic properties

As their analogues, the coordination complexes herein synthesized self-assemble into columnar hexagonal liquid crystalline mesophases, identified by typical fan-shaped focal texture with homeotropic zones (Figure 3).

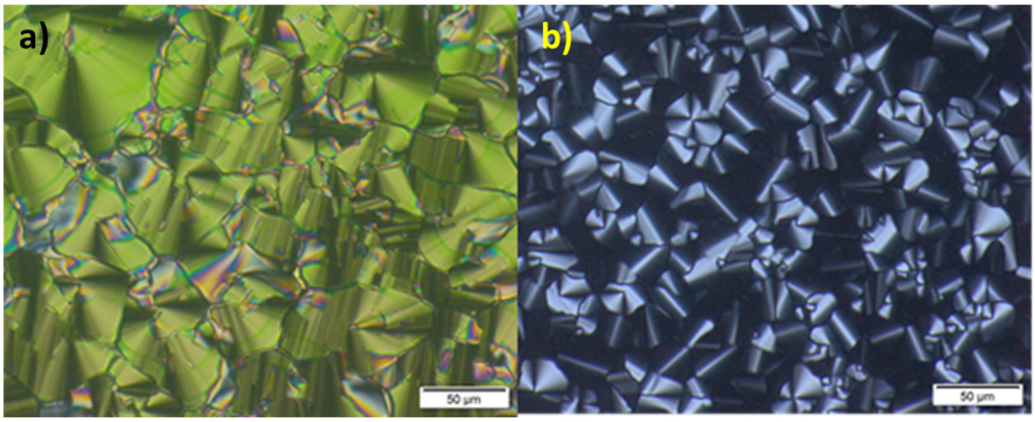

Figure 3. POM micrograph of the textures developed by a) **Zn$_1$Fe$_2$** on first cooling, at 30°C, magnification 20x and b) **Zn$_2$Fe$_4$** on first cooling at 100°C, magnification 20x.

The introduction of the ferrocene unit in the liquid-like region of the columnar structure decreases the transition temperatures and the order degree like for parent compound previously reported [19]. Indeed, while complex **Zn$_1$** arranged into a three-dimensional columnar hexagonal mesophase (M$_{hex}$) from room temperature to 229°C [21], complexes **Zn$_1$Fe$_2$** and **Zn$_2$Fe$_4$** self-assemble into classical 2D Col$_{hex}$, with lower isotropisation temperatures (Figures 4 and 5).

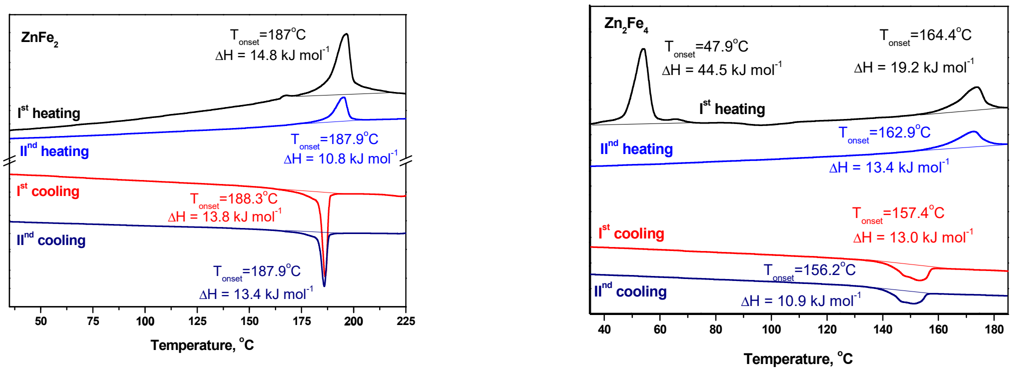

(**a**) (**b**)

Figure 4. DSC thermograms of: (**a**) complex **Zn$_1$Fe$_2$** and (**b**) complex **Zn$_2$Fe$_4$**.

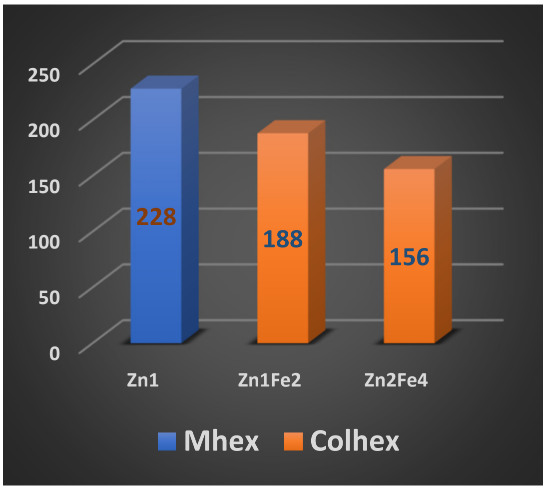

Figure 5. Bar graph with mesomorphic properties of complexes.

2.3. Photophysics

The photophysical properties of the complexes were firstly recorded from dilute dichloromethane solutions (see Figure 6).

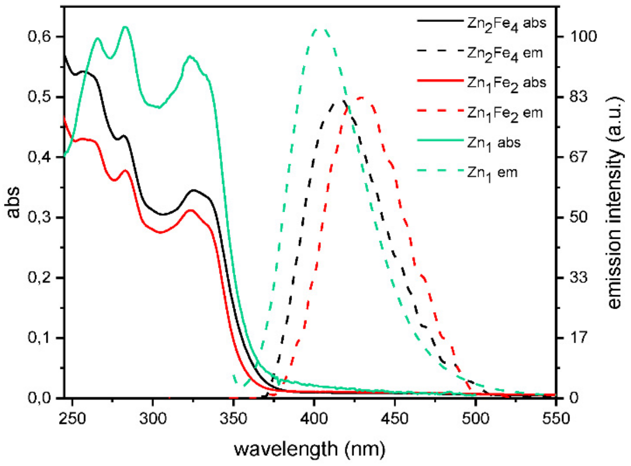

Figure 6. Normalized absorption and emission spectra of 1.0 E-5 M dichloromethane solution of the complexes.

The absorption spectra are very similar: they all have three main bands each accompanied by shoulders. The first two bands, positioned at 260 and 283 nm respectively, are attributed to ligand-centered (LC) transitions located on the terpyridine fragment (see Figures S5, S6, S7, S8 in SI) [21], while the third band, positioned at 325 nm, is attributed to a charge transfer transition from the gallate to the terpyridine ligand (LLCT) [43]. All complexes are fluorescent, showing a band ranging from 405 to 428 nm, depending on the complex, but due for all to deactivation from LLCT state. To explore the effect of the polarity of the environment on the photophysical properties, nine solutions were prepared by adding increasing amounts of methanol to the 1.0 E-5 M dichloromethane solution of **Zn_2Fe_4**, keeping the volume constant. Absorption and emission spectra are reported in Figure 7.

The absorption bands, considering the experimental uncertainty, show a constant trend: as the methanol fraction increases, their intensity increases. The emission band instead undergoes a bathochromic shift as the percentage of methanol increases, while the emission intensity increases as the alcoholic fraction increases, especially when this becomes greater than 50%.

To verify whether these variations could depend on the concentration of the solutions, the absorption and emission spectra were collected in the two pure solvents at different concentrations, but only a linear growth of the spectral intensities with concentration was observed.

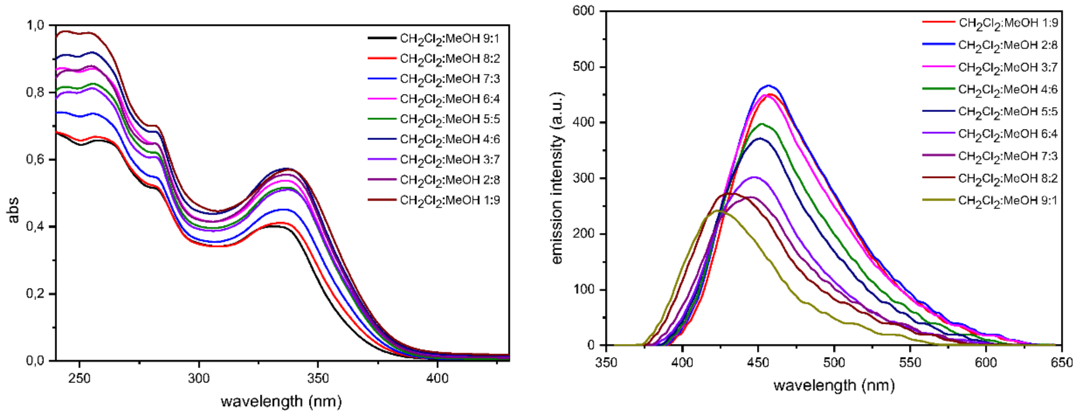

Figure 7. Absorption (left) and emission (right) spectra of **Zn_2Fe_4** in 1.0 E-5M dichloromethane solution recorded at increasing amounts of methanol.

doi:10.20944/preprints202312.0457.v1

The photophysical properties of **Zn$_2$Fe$_4$** were determined also in the mesophase, by obtaining a film drop casted from a concentrated DCM solution on a glass plate. The solvent was evaporated, the film was dried under vacuum and thermally treated by heating it until the isotropic phase and then slowly cooled down. The order was checked by POM (Figure 8).

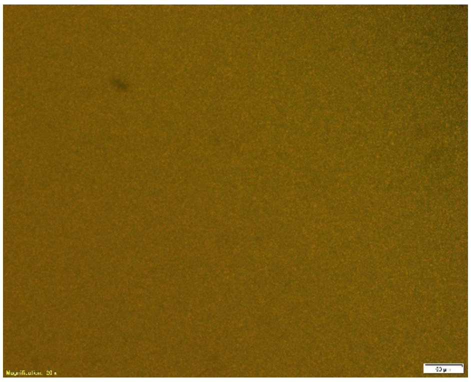

Figure 8. POM micrograph of the **Zn$_2$Fe$_4$** film thermally treated: birefringent texture indicates liquid crystalline order.

The absorption spectrum in mesophase is reported in Figure 9a. Compared to the absorption spectrum recorded in DCM solution, it shows additional bands at 490 and 580 nm due to the formation of the supramolecular mesogenic structure, which leads to an energy lowering of the electronic states compared to the isolated molecule. These electronic states are primarily non-radiatively deactivated, because mesophase is not luminescent if excited on these electronic levels. However, by exciting mesophase sample at 350 nm (i.e. on the levels attributed to the isolate molecules) an emission band peaked at 430 nm (Figure 9b), attributable by comparison with solution sample (Figure 7) to the isolated molecule, has been recorded. This behavior seems to indicate, in the mesophase structure, different surroundings of the molecules, causing the presence of molecules which, not iterating significantly, show an emission identical to that of the isolated molecule, while, at smaller distances, they give rise to π–π stacking interactions, which do not present emission, but are responsible for the absorption bands around 580 nm.

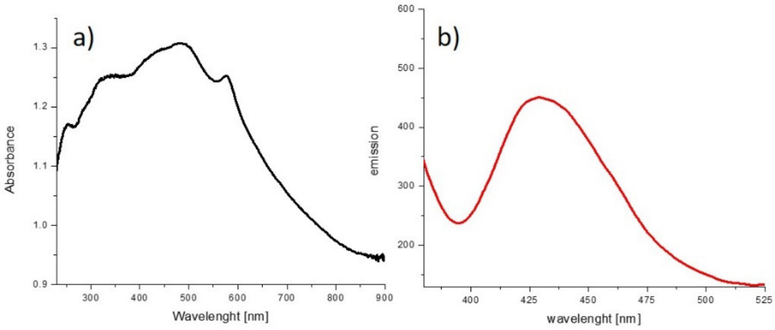

Figure 9. a) Absorption and b) emission (excited at 350 nm) of the ordered **Zn$_2$Fe$_4$** film.

3. Discussion

The introduction of a second metal center in the aliphatic regions of complex **Zn$_1$** increased the symmetry of the mesophase and decreased transition temperatures, as expected when compared with the parent compound reported previously [19]. However, in condensed "soft" phases the properties of the complexes depend not only on the molecular structure, but also are influenced on the supramolecular arrangements in the mesophase, and the molecular environment. Hence, the influence of the polarity of the media were studied in solution.

The variation in the emission intensity as the polarity of the solvent varies, in principle, can be due to various non-mutually exclusive factors: the formation of aggregates (due to a different solubility in the new solvent), and the effect of refractive index of the solvent; finally, it is necessary to consider the possibility that by modifying the solvent specific interactions of the fluorophore with the solvent can be established, for example formation of hydrogen bonds, acid-base chemistry or charge transfer interactions [44]. The formation of aggregates as methanol is added can be excluded since, if Zn_2Fe_4 was prone to form aggregates that modify its photophysics, such structures should also form as the concentration increases; but no such changes in absorption or luminescence were observed as the concentration of the complex varied in either methanol or dichloromethane. The absence of variations in the shape of the absorption and emission spectra allows us to exclude the presence of specific solvent/complex interactions. Based on this, the increase in the intensity of the absorption and emission spectrum and the red shift of the luminescence that are observed with the increase in the alcohol fraction can be attributed to the increase in the polarity of the surrounding environment.

When passing to the condensed liquid crystalline state from solution, the absorption properties change significantly, leading to the formation of lower energy states. These states are not emissive, the quenching of the emission being attributable to the formation of non-emissive aggregates, but also to the change in the polarity of the molecular surroundings. However, some emission arising from the presence of "isolated" molecules can be detected, similar to the emission in DCM solution.

4. Materials and Methods

All precursor materials commercially available and solvents were used as received without further purification.

Ferrocene, anhydrous $AlCl_3$, $NaBH_4$, anhydrous dichloromethane and tetrahydrofuran were purchased from Sigma Aldrich, while hexane and ethyl acetate were purchased from Carlo Erba; HPLC-grade dichloromethane was purchased from Honeywell.

A Bruker - Fourier 80 Research FT-NMR Benchtop 80 MHz spectrometer was used to record ^1H NMR experiments in $CDCl_3$. Elemental analysis was carried out using a Flash 2000 microanalyser from Thermo Fisher Scientific. Zn(II)% was determined using a Sens AA flame atomic absorption spectrometer (GBC Scientific Equipment, Braeside, Australia) equipped with a zinc hollow cathode lamp. The detection limit was 0.4–1.5 mg/L and the integration time 3 s in air–acetylene mixture. An average absorbance value of two determinations was reported.

Optical textures of the mesophases were observed with an Olympus BX53M polarizing microscope (POM) equipped with a Linkam hot stage and an Olympus UC90 camera DSC traces were recorded with a Q1000 apparatus from TA Instruments calibrated with indium; three heating/cooling cycles were performed for each sample, with a heating and cooling rate of 10°C/min.

Spectrofluorimetric grade solvents were used for the photophysical investigations in solution, at room temperature. An Agilent Cary 60 spectrophotometer was employed to obtain the absorption spectra, while the corrected emission spectra, all confirmed by excitation ones, were recorded with a on a Perkin-Elmer Model LS 55 apparatus (PerkinElmer, Inc./UK Model LS 55, Waltham, MA, USA), using 1 cm path length cells. Electronic spectra in mesophase of complex $\mathbf{Zn_2Fe_4}$ were recorded using a V-650 double-beam spectrophotometer with a photomultiplier tube detector, 60 mm integrating sphere coated with barium sulfate.

4.1. Synthesis of ligands

L1: 4-(2,6-di(pyridin-2-yl)pyridin-4-yl)phenol: 4'-(4-methoxyphenyl)-2,2':6',2''-terpyridine (10.9 g, 32.1 mmol) were refluxed in an excess of 48% HBr/ CH_3COOH for 24 h, then cooled to room temperature and neutralized with NaOH 20 %. The precipitate was filtered off and washed with water, resulting in a pale grey solid (10.21 g, 31.3 mmol, 95 %).

^{1}H-NMR (300 MHz, DMSO-d_6, δ- ppm): 8.78- 8.70 (d, 2H), 8.68-8.59(d, 4H), 8.07- 7.95 (td, 2H), 7.82 -7.61(m, 2H), 7.58- 7.43 (m, 2H), 7.00- 6.95(dd, 2H).

L2: A mixture of 4-(2,6-di(pyridin-2-yl)pyridin-4-yl)phenol (1.00 g, 3.074 mmoli) and K_2CO_3 (1.27 g, 9.189 mmol) in 50 mL DMF was heated to 65°C, then n-bromododecane (2.02 g, 6.148 mmol) in 5 mL DMF was added to the mixture. The reaction mixture was stirred at 80°C for 24 hours, cooled to room temperature and filtered. The mixture was diluted with water (300 mL) and extracted with DCM (4 x 100 mL). The combined organic layers were washed with H_2O (5 x 100 mL), NH_4Cl (100 mL) saturated and NaCl saturated (100 mL). Recrystallization from CH_2Cl_2/MeOH afforded the pure product as a white powder (1.70 g, 2.09 mmol, 68%).

^{1}H-NMR (300 MHz, $CDCl_3$, δ- ppm): 8.65 (overlapped peaks, 12H), 7.78 (overlapped peaks, 8H), 7.30 (t, 4H), 7.65 (d, $^3J = 8.5$ Hz, 4H), 3.94 (t, $^3J = 6.1$ Hz, 4H), 3.51 (m, 4H), 1.30 (m, 16H).

4.2. Synthesis of complexes

To a solution of **galFe** [3] (0.200 g, 0.237 mmol) in 15 mL $CHCl_3$ was added dropwise an ethanolic solution of NaOH (0.0095 g, 0.237 mmol). The reaction mixture was stirred at room temperature for 30 minutes, then $ZnCl_2$ (0.016 g, 0.119 mmol) dissolved in the minimum amount of EtOH was added dropwise. After 60 minutes of stirring, the solvent was removed under reduced pressure to give a pale orange residue, which was used without any purifications in the next step.

The residue was dissolved in 10 mL of $CHCl_3$, a solution of ligand **Ln** (0.119 mmol) in 10 mL $CHCl_3$ was added dropwise resulting in a brown solution which was stirred at r.t for 24 hours. After that the solvents were removed under reduced pressure. The complexes were obtained as yellow solids as following: **$ZnFe_2$**: recrystallisation from acetone (64%). Anal. Calcd. for $C_{126}H_{183}Fe_2N_3O_{11}Zn$ (2092.89 g·mol^{-1}): C, 72.31; H, 8.81; N, 2.01. Found: C, 72.40; H, 8.79; N, 2.02%. AAS: Zn% calcd.: 3.12, found: 3.15. ^{1}H NMR (80 MHz, $CDCl_3$, δ/ppm) 8.97 (d, $^3J = 4.9$ Hz ,2H, H^1), 8.17 (overlapped peaks, 4H, $H^{5,4}$), 7.71 (overlapped peaks, 4H, $H^{6,3}$), 7.35 (overlapped peaks, 2H, $H^{2,8,8'}$), 4.03 (overlapped peaks, 33H, -OC*H*$_2$-, -OC*H*$_3$, H^{Fc}), 2.32 (m, 4H, -C*H*$_2$-Fc), 1.75 – 1.10 (overlapped peaks, 122 H), 0.92 (t, $J = 4.9$ Hz, 12H).

FT-IR (KBr, cm^{-1}): $\nu_{C\text{-}H,Fc}$ (3080), $\nu_{CH2,as}$ (2924), $\nu_{CH2,s}$ (2863), 1625 ($\nu_{as\ COO\text{-}}$), 1360 ($\nu_{s\ COO\text{-}}$): $\nu = 265$ cm^{-1}, $\nu_{C=O}$ (1578), $\nu_{C\text{-}O}$ (1245, 1106), out of-plane vibration of Fc cyclopentadiene (1002, 914), $\nu_{ring\text{-}Fe,\ Fc}$ (486).

Zn_2Fe_4: recrystallisation hexane/EtOH (70%). Anal. Calcd. for $C_{262}H_{384}Fe_4N_6O_{22}Zn_2$ (4324.04 g·mol^{-1}): C, 72.77; H, 8.95; N, 1.94. Found: C, 72.71; H, 9.01; N, 1.95%. AAS: Zn% calcd.: 3.02, found: 3.03. ^{1}H NMR (80 MHz, $CDCl_3$, δ/ppm) 8.91 (d, $^3J = 4.6$, 4H, H^1), 8.20 (overlapped peaks, 8H, $H^{5,4}$), 7.64 (overlapped peaks, 8H, $H^{6,3}$), 7.28 (overlapped peaks, 12H, $H^{2,8,8'}$), 6.76 (d, $^3J = 8.3$ Hz, 4H, H^7), 3.96 (overlapped peaks, 64 H, OC*H*$_2$, H^{Fc}), 2.20 (m, 8H, -C*H*$_2$-Fc), 1.75 – 1.10 (overlapped peaks, 252 H), 0.85 (t, $J = 4.9$ Hz, 24H).

FT-IR (KBr, cm^{-1}): $\nu_{C\text{-}H,Fc}$ (3091), $\nu_{CH2,as}$ (2924), $\nu_{CH2,s}$ (2863), 1620 ($\nu_{as\ COO\text{-}}$), 1362 ($\nu_{s\ COO\text{-}}$): $\nu = 258$ cm^{-1}, $\nu_{C=O}$ (1594), $\nu_{C\text{-}O}$ (1218, 1114), out of-plane vibration of Fc cyclopentadiene (1002, 902), $\nu_{ring\text{-}Fe,\ Fc}$ (483).

5. Conclusions

The study of the photophysical properties of liquid-crystalline compounds starts from their characterization in solution. However, before comparing the behavior of these compounds in solution and in mesophase, it is necessary to study the effect of the environment on photophysics. In the liquid-crystalline phase, in fact, intermolecular interactions become important, but sometimes the effects of the change in polarity of the environment are neglected. In this work we wanted to conduct a preliminary study of the photophysics of a hetero-polymetallic mesogenic compound by varying the polarity of the solvent, and observing how an increase in polarity leads to an increase in emission and its bathochromic shift, in the absence of the formation of aggregates that could influence photophysics. However, by the formation of aggregates, the quenching of the emission in mesophase was obtained and only a weak emission arising from "isolated" molecules that are probably not forming the columnar structures was observed. By synthesizing hetero-polynuclear coordination complexes, new and synergistic properties can be expected. However, the design of highly luminescent metallomesogens has to consider several factors that influences the emission properties in condensed states including the polarity of the molecular environment.

Supplementary Materials: The following supporting information can be downloaded at the website of this paper posted on Preprints.org, Figure S1: Absorption spectrum of **L1** in dichloromethane solution; Figure S2:

Emission spectrum of L1 in dichloromethane solution; Figure S3: Absorption spectrum of L2 in dichloromethane solution; Figure S4: Emission spectrum of L2 in dichloromethane solution.

Author Contributions: Conceptualization, E.I.S and M.L.D.; methodology, A.A.A., E.I.S and M.L.D.; investigation, A.A.A., A.C., C.C. and E.P.; resources, A.A.A.; data curation, E.I.S and M.L.D.; writing—original draft preparation, A.A.A., E.I.S and M.L.D.

Funding: This work was supported by a grant of the Ministry of Research, Innovation and Digitization, CNCS/CCCDI – UEFISCDI, project number PN-III-P1-1.1-PD-2021-0427, within PNCDI III.

Institutional Review Board Statement: Not applicable

Informed Consent Statement: Not applicable

Data Availability Statement: Not applicable.

Acknowledgments: We acknowledge the Romanian Academy, Program 4 and the project ROOPENSCREEN, MySMIS code: 127952, Contract no. 371/20.07.2020, co-financed by European Regional Development Fund through the Competitiveness Operational Program 2014-2020, for support. This work was supported by a grant of the Ministry of Research, Innovation and Digitization, CNCS/CCCDI – UEFISCDI, project number PN-III-P1-1.1-PD-2021-0427, within PNCDI III.

Conflicts of Interest: The authors declare no conflict of interest.

Sample Availability: Samples of the compounds: ligands **L1** and **L2** and coordination complexes **Zn$_1$**, **Zn$_1$Fe$_2$** and **Zn$_2$F$_4$** are available from the authors.

References

1. Bizzarri, C.; Spuling, E., Knoll, D.M.; Volz, D.; Bräse, S. Sustainable metal complexes for organic light-emitting diodes (OLEDs). *Coord. Chem. Rev.* **2018**, *373*, 49–82.
2. Zhang, Q.-C.; Xiao, H.; Zhang, X.; Xu, L.-J.; Chen Z.-N. Luminescent oligonuclear metal complexes and the use in organic light-emitting diodes. *Coord. Chem. Rev.* **2019**, *378*, 121-133.
3. Housecroft, C.E.; Constable, E.C. TADF: Enabling luminescent copper(I) coordination compounds for light-emitting electrochemical cells. *J. Mater. Chem. C* **2022**, *10*, 4456-4482.
4. Dey, N.; Haynes, C.J.E. Supramolecular Coordination Complexes as Optical Biosensors. *ChemPlusChem* **2021**, *86*, 418–433.
5. Pobłocki, K.; Drzeżdżon, J.; Kostrzewa, T.; Jacewicz, D. Coordination Complexes as a New Generation Photosensitizer for Photodynamic Anticancer Therapy. *Int. J. Mol. Sci.* **2021**, *22*, 8052.
6. Consiglio, G.; Oliveri, I.P.; Failla, S.; Di Bella, S. On the Aggregation and Sensing Properties of Zinc(II) Schiff Base Complexes of Salen-Type Ligands. *Molecules* **2019**, *24*, 2514.
7. Cuerva, C.; Cano, M.; Lodeiro, C. Advanced Functional Luminescent Metallomesogens: The Key Role of the Metal Center. *Chem. Rev.* **2021**, *121*, 12966–13010.
8. Diana, R.; Caruso, U.; Panunzi, B. Stimuli-Responsive Zinc (II) Coordination Polymers: A Novel Platform for Supramolecular Chromic Smart Tools. *Polymers* **2021**, *13*, Art. No. 3712.
9. Kobayashi, A.; Kato, M. Stimuli-Responsive Luminescent Copper(I) Complexes for Intelligent Emissive Devices. *Chem. Letters* **2017**, *46*, 154-162.
10. Li, K.; Chen, Y.; Wang, J.; Yang C. Diverse emission properties of transition metal complexes beyond exclusive single phosphorescence and their wide applications. *Coord. Chem. Rev.* **2021**, *433*, 213755.
11. Szerb, E.I.; Crispini, A.; Aiello, I.; La Deda, M. in *Springer Handbook of Inorganic Photochemistry*, Bahnemann D.W., Patrocinio A.O.T. Eds. Part XII: Inorganic Materials for Optoelectronics, 62: Liquid Crystals, Section editor: Eli Zysman-Colman. **2022**, pp. 1811-1848.
12. De Sio, L.; Ricciardi, L.; Serak, S.; La Deda, M.; Tabiryan N.; Umeton C. Photo-sensitive liquid crystals for optically controlled diffraction gratings. J. *Mater. Chem.* **2012**, *22*, 6669-6673.
13. Panicker, R.R.; Sivaramakrishna, A. Remarkably flexible 2,2':6',2"-terpyridines and their group 8-10 transition metal complexes - Chemistry and applications. *Coord. Chem. Rev.* **2022**, *459*, 214426.
14. Saleh, D.A.; Rana, U.; Higuchi, M.; Sosnik, A. Luminescent amphiphilic nanogels by terpyridine-Zn(II) complexation of polymeric micelles. *Mater. Today Chem.* **2020**, *18*, 100359.
15. Yan, Y.; Yin, G.-Q.; Khalife, S.; He, Z.-H.; Xu, C.; Li, X. Self-assembly of emissive metallocycles with tetraphenylethylene, BODIPY and terpyridine in one system. *Supramol. Chem.* **2019**, *31*, 597-605
16. Singh, V.D.; Dwivedi, B.K.; Paitandi, R.P.; Kumar, Y.; Pandey, D.S. Effect of substituents on photophysical and aggregation behaviour in quinoline based bis-terpyridine Zn(II) complexes. *Inorganica Chim. Acta* **2019**, *487*, 24-30.

17. Li, M.; Jiang, S.; Zhang, Z.; Hao, X.-Q.; Jiang, X.; Yu, H.; Wang, P.; Xu, B.; Wang, M.; Tian, W. Tetraphenylethylene-Based Emissive Supramolecular Metallacages Assembled by Terpyridine Ligands. *CCS Chem*. **2020**, *2*, 337–348.
18. Jung, S.H.; Kwon, K.-Y.; Jung, J.H. A turn-on fluorogenic Zn(II) chemoprobe based on a terpyridine derivative with aggregation-induced emission (AIE) effects through nanofiber aggregation into spherical aggregates. *Chem. Commun*. **2015**, *51*, 952-955.
19. Popa, E.; Andelescu, A.A.; Ilies, S.; Visan, A.; Cretu, C.; Scarpelli, F.; Crispini, A.; Manea, F.; Szerb, E.I. Hetero-Bimetallic Ferrocene-Containing Zinc(II)-Terpyridyl-Based Metallomesogen: Structural and Electrochemical Characterization. *Materials* **2023**, *16*, 1946.
20. Andelescu, A.A.; Ilies (b. Motoc), S.; Cretu, C.; Popa, E.; Marinescu, S.; Heinrich, B.; Manea, F.; Negrea, S.; Donnio, B.; Szerb E.I. Pentacoordinated Liquid Crystalline Zn(II) Complex Organized in Smectic Mesophase: Synthesis, Structural and Electrochemical Properties. *Appl. Sci*. **2022**, *12*, 8306.
21. La Deda, M.; Di Maio, G.; Candreva, A.; Heinrich, B.; Andelescu, A.A.; Popa, E.; Voirin, E.; Badea, V.; Amati, M.; Costisor, O.; Donnio, B.; Szerb, E.I. Very intense polarized emission in self-assembled room temperature metallomesogens based on Zn(II) coordination complexes: an experimental and computational study. *J. Mater. Chem. C* **2022**, *10*, 115-125.
22. Lakshmanana, R.; Shivaprakash, N.C.; Sindhu, S. Switching from sky blue to deep green fluorescent Zn(II) complexes for OLEDs applications. *J. Lumin*. **2018**, *196*, 136–145.
23. Winter, A.; Friebe, C.; Chiper, M.; Schubert, U. S.; Presselt, M.; Dietzek, B.; Schmitt, M.; Popp, J. Synthesis, Characterization, and Electro-Optical Properties of Zn^{II} Complexes with -Conjugated Terpyridine Ligands. *ChemPhysChem* **2009**, *10*, 787-798.
24. Singh, V.D.; Singh, R.S.; Paitandi, R.P.; Dwivedi, B.K.; Maiti, B.; Pandey, D.S. Solvent Dependent Self-Assembly and AIE in Zn(II) Complexes Containing Phenothiazine Based Terpyridine Ligand and Its Efficacy in Pyrophosphate Sensing. *J. Phys. Chem. C* **2018**, *122*, 5178–5187.
25. Kaushik, R.; Ghosh, A.; Jose, D. A. Simple terpyridine based Cu(II)/Zn(II) complexes for the selective fluorescent detection of H_2S in aqueous medium. *J. Lumin*. **2016**, *171*, 112–117.
26. Das, D.; Sarkar, P.; Kumar, A.H.U.; Sutradhar, S.; Kotakonda, M.; Lokanath, N.K.; Ghosh, B.N. Nanomolar pyrophosphate detection in water using a zinc-terpyridine receptor and its applications in antiproliferative and antioxidant activity. *J. Photochem. Photobiol., A* **2023**, *441*, 114726.
27. Velugula, K.; Chinta, J.P. Silver nanoparticles ensemble with Zn(II) complex of terpyridine as a highly sensitive colorimetric assay for the detection of Arginine. *Biosens. Bioelectron*. **2017**, *87*, 271-277.
28. Chao, D.B.; Ni, S.T. Nanomolar pyrophosphate detection and nucleus staining in living cells with simple terpyridine-Zn(II) complexes. *Sci. Rep*. **2016**, *6*, 26477.
29. Xiao, B.W.; Zhang, Q.Q.; Huang, C.Z.; Li, Y.F. Luminescent Zn(II)-terpyridine metal-organic gel for visual recognition of anions. *RSC Adv*. **2015**, *5*, 2857-2860.
30. Shen, Y.; Shao, T.; Fang, B.; Du, W.; Zhang, M.Z.; Liu, J.J.; Liu, T.Y.; Tian, X.H.; Zhang, Q.; Wang, A.D.; Yang, J.X.; Wu, J.Y.; Tian, Y.P. Visualization mitochondrial DNA in living cells under superresolution microscopy using thiophene-based terpyridine Zn(II) complexes. *Chem. Commun*. **2018**, *54*, 11288-11291.
31. Hsu, T.W.; Hsu, H.C.; Chan, H.Y.; Fang, J.M. A Terpyridine Zinc Complex for Selective Detection of Lipid Pyrophosphates: A Model System for Monitoring Bacterial O- and N-Transglycosylations. *J. Org. Chem*. **2020**, *85*, 12747-12753.
32. Zhang, J.F.; Qiu, Q.X.; Xiang, Q.; Ren, S.M. Two Zn(II)-organic frameworks based on "V"-shaped terpyridine ligand and dicarboxylic ligands: Fascinating architectures and efficient luminescent aqueous-phase dual-responsive detection. *J. Solid State Chem*. **2021**, *294*, 121849.
33. Negrea, S.; Andelescu, A.A.; Ilies (b. Motoc), S.; Cretu, C.; Cseh, L.; Rastei, M.; Donnio, B.; Szerb, E.I.; Manea, F. Design of Nanostructured Hybrid Electrodes Based on a Liquid Crystalline Zn(II) Coordination Complex-Carbon Nanotubes Composition for the Specific Electrochemical Sensing of Uric Acid, *Nanomaterials* 2022, *12*, 4215.
34. Jiang, Q.; Zhu, J.; Zhang, Y.; Xiao, N.; Guo, Z. DNA binding property, nuclease activity and cytotoxicity of Zn(II) complexes of terpyridine derivatives. *Biometals* **2009**, *22*, 297–305.
35. Ma, Z.; Cao, Y.; Li, Q.; Guedes da Silva, M.F.C.; Fraústo da Silva, J.J.R.; Pombeiro, A.J.L. Synthesis, characterization, solid-state photo-luminescence and anti-tumor activity of zinc(II) 4-phenyl-terpyridine compounds. J. Inorg. Biochem. 2010, 104, 704–711.
36. Busto, N.; Carrión, M.C.; Montanaro, S.; de Greñu, B.D.; Biver, T.; Jalón, F.A.; Manzano, B.R.; García, B. Targeting G-Quadruplex structures with Zn(II) terpyridine derivatives: a SAR study. *Dalton Trans*. **2020**, *49*, 13372-13385.
37. Gao, E.J.; Feng, Y.H.; Su, J.Q.; Meng, B.; Jia, B.; Qi, Z.Z.; Peng, T.T.; Zhu, M.C. Synthesis, characterization, DNA binding, apoptosis and molecular docking of three Mn(II), Zn(II) and Cu(II) complexes with terpyridine-based carboxylic acid. *Appl. Organomet. Chem*. **2018**, *32*, e4164.

38. Wang, H.; Cai, F.Z.; Feng, D.X.; Zhou, L.; Li, D.; Wei, Y.; Feng, Z.J.; Zhang, J.; He, J.; Wu, Y.J. Synthesis, crystal structure, photophysical property and bioimaging application of a series of Zn(II) terpyridine complexes. *J. Mol. Struct*. **2019**, *1194*, 157e162.
39. Kong, C.C.; Peng, M.H.; Shen, H.; Wang, Y.M.; Zhang, Q.; Wang, H.; Zhang, J.; Zhou, H.P.; Yang, J.X.; Wu, J.Y.; Tian, Y.P. A novel D-A type terpyridine-based carbazole Zn(II) complex with enhanced twophoton absorption and its bioimaging application. *Dyes Pigm*. **2015**, *120*, 328-334.
40. Du, W.; Pan, D.Y.; Xiang, P.; Xiong, C.Y.; Zhang, M.Z.; Zhang, Q.; Tian, Y.P.; Zhang, Z.P.; Chen, B.; Luo, K.; Gong, Q.Y.; Tian, X.H. Terpyridine Zn(II) Complexes with Azide Units for Visualization of Histone Deacetylation in Living Cells under STED Nanoscopy. *ACS Sensors* **2021**, *6*, 3978-3984.
41. Kröhnke, F. Synthesis 1976, 1-24.
42. Chen, F.; Tian, Y. -K.; Chen, Y. Chem. Asian J. 2018, 13, 3169 – 3172.
43. Andelescu, A.-A.; Heinrich, B.; Spirache, M. A.; Voirin, E.; La Deda, M.; Di Maio, G.; Szerb, E. I.; Donnio, B.; Costisor O. Playing with PtII and ZnII Coordination to Obtain Luminescent Metallomesogens. *Chem. Eur. J*. **2020**, *26*, 4850 – 4860.
44. Lakowicz, J.R. (1999). Principles of Fluorescence Spectroscopy. Springer, Boston, MA.